Paper Number: **2606**

Title: **In Search of a Time Efficient Approach to Crack and Delamination Growth Predictions in Composites**

Authors: **Ronald Krueger**
Nelson Carvalho

ABSTRACT

Analysis benchmarking was used to assess the accuracy and time efficiency of algorithms suitable for automated delamination growth analysis. First, the Floating Node Method (FNM) was introduced and its combination with a simple exponential growth law (Paris Law) and Virtual Crack Closure technique (VCCT) was discussed. Implementation of the method into a user element (UEL) in Abaqus/Standard® was also presented. For the assessment of growth prediction capabilities, an existing benchmark case based on the Double Cantilever Beam (DCB) specimen was briefly summarized. Additionally, the development of new benchmark cases based on the Mixed-Mode Bending (MMB) specimen to assess the growth prediction capabilities under mixed-mode I/II conditions was discussed in detail. A comparison was presented, in which the benchmark cases were used to assess the existing low-cycle fatigue analysis tool in Abaqus/Standard® in comparison to the FNM-VCCT fatigue growth analysis implementation. The low-cycle fatigue analysis tool in Abaqus/Standard® was able to yield results that were in good agreement with the DCB benchmark example. Results for the MMB benchmark cases, however, only captured the trend correctly. The user element (FNM-VCCT) always yielded results that were in excellent agreement with all benchmark cases, at a fraction of the analysis time. The ability to assess the implementation of two methods in one finite element code illustrated the value of establishing benchmark solutions.

INTRODUCTION

Over the past two decades, the use of fracture mechanics has become common practice for characterizing the onset and growth of delaminations [1, 2]. Delamination onset or growth is predicted by comparing the calculated strain energy release rate components to interlaminar fracture toughness properties measured over a range from pure mode I loading to pure mode II loading [2].

Ronald Krueger, Nelson Carvalho, National Institute of Aerospace, 100 Exploration Way, Hampton, VA, 23666. This work was performed at the Durability, Damage Tolerance and Reliability Branch, MS 188E, NASA Langley Research Center, Hampton, VA, 23681, U.S.A.

The virtual crack closure technique (VCCT) is widely used for computing energy release rates, using results from continuum (2D) and solid (3D) finite element (FE) analyses, and is able to supply the mode separation required by a mixed-mode fracture criterion [3, 4]. The virtual crack closure technique was recently implemented into several commercial finite element codes. Other new methods for analyzing composite delamination may also be incorporated into finite element codes in the future. Thus, the need to compare these codes to benchmark examples is necessary, since each code requires specific input parameters unique to its implementation. These parameters are unique to the numerical approach chosen and do not reflect real *physical* differences in delamination behavior.

An approach for assessing the mode I, and mixed-mode I/II, delamination propagation capabilities in commercial finite element codes under static loading was recently presented and demonstrated for Abaqus/Standard® [5]. The approach was then extended to allow the assessment of the delamination growth prediction capabilities under fatigue in commercial finite element codes [6]. This approach was similar to the static case, for which benchmark results were created manually first. Second, using a commercial code, a delamination in a finite element model was allowed to grow. In general, good agreement between the results obtained from the FE propagation and growth analysis and the benchmark results could be achieved when the appropriate input parameters were selected. However, the analyses were not time efficient, since even models of simple specimens required many days of computation time [6].

The objective of the present study is to use benchmark examples to assess accuracy and time efficiency of approaches and algorithms for automated delamination growth analysis which can be implemented in commercial FE codes. First, the Floating Node Method (FNM) and its combination with VCCT is introduced. Second, the combination of the FNM with a simple exponential growth law (Paris Law) and VCCT, as well as the implementation in Abaqus/Standard®, is discussed [7]. Third, an existing benchmark case for the assessment of growth prediction capabilities under pure mode I conditions is introduced. Fourth, the development of new benchmark cases to assess the growth prediction capabilities under mixed-mode I/II conditions is discussed. Fifth, a comparison is presented, where the benchmark cases were used to assess the existing low-cycle fatigue analysis tool in Abaqus/Standard® in comparison to the FNM-VCCT fatigue growth analysis implementation. The significance of the findings is discussed at the end of the study.

MODELING FATIGUE DAMAGE PROPAGATION USING THE FLOATING NODE METHOD COMBINED WITH VCCT

Floating Node Method and element based VCCT

The Floating Node Method (FNM) has been proposed in [8] to represent multiple discontinuities in solids in a mesh independent fashion. One of the main advantages of the method is the simplicity with which multiple cracks and their connection can be accommodated within an element in a mesh-independent fashion.

In the present work, the 3D extended interface element developed in [7] is used to represent delamination. This element is capable of representing both delaminations and matrix cracks with any in-plane orientation; further details are provided in [7].

To determine energy release rates, the FNM is coupled with VCCT applied at the element level [7]. In this implementation of VCCT, shape functions of interface elements are used to obtain tractions and openings at integration points, and compute energy release rates for a given element. This procedure is used instead of the typical nodal based VCCT, primarily for convenience when coupling VCCT with the crack representation performed using the FNM.

Delamination propagation

Delaminations are assumed to propagate following a Paris Law given by:

$$\frac{\mathrm{d}a}{\mathrm{d}N} = c(G_{max})^n \tag{1}$$

where G_{max} corresponds to the maximum energy release rate obtained at peak load, and can be determined by:

$$G_{max} = G_{n-max} + G_{s-max} + G_{t-max} \tag{2}$$

in which G_{n-max} is the energy release rate associated with the opening mode, and G_{s-max} and G_{t-max} are energy release rates associated with shearing obtained in orthogonal in-plane directions. The coefficient c and exponent n are assumed to be a function of mode-mixity β, which is given by:

$$\beta = \frac{G_{s-max} + G_{t-max}}{G_{max}} \tag{3}$$

An overview of the fatigue algorithm implemented is provided in Figure 1. At a given step s, the energy release rate, mode-mixity, and the growth rate are determined for each element e_k at the crack front. A binary failed/not failed approach is implemented. The uncracked area $A_{uc}^{e_k}$ is used as an internal state variable that tracks crack accumulation for the elements at the crack front that do not fail in a given step. An element is considered to fail if its uncracked area $A_{uc}^{e_k}$ is reduced below a fraction f of the original area:

$$A_{uc}^{e_k}\big|_{s+1} < f A^{e_k} \tag{4}$$

Otherwise, the element is considered to be pristine. In the present study, $f = 0.1$ is used. Hence, before damage:

$$A_{uc}^{e_k} = A^{e_k} \tag{5}$$

where A^{e_k} corresponds to the area of the element. The cycles needed to fail each element at the crack front, at step s, can be obtained as:

$$\Delta N^{e_k} = \frac{A_{uc}^{e_k}\big|_s}{\left(\frac{\mathrm{d}a}{\mathrm{d}N}\right)^{e_k} l^{e_k}} \tag{6}$$

where length l^{e_k} is given as the length of the common edge between the element e_k and the adjacent element used in the G_{max} calculation; further details are provided in [7]. Next, the minimum number of cycles (ΔN_{min}) needed to fail an element in the model is determined:

$$\Delta N_{min} = \min\{\Delta N^{e_1}, \Delta N^{e_2}, \ldots\} \tag{7}$$

and assumed to correspond to the cycle increment registered in the step s:

$$\Delta N_{inc} = \Delta N_{min} \tag{8}$$

Knowing the cycle increment and the growth rate, the crack increment, ΔA^{e_k}, can be calculated from:

$$\Delta A^{e_k} = l^{e_k} \left(\frac{\mathrm{d}a}{\mathrm{d}N}\right)^{e_k} \Delta N_{inc} \tag{9}$$

and an updated uncracked area obtained as

$$A_{uc}^{e_k}\big|_{s+1} = A_{uc}^{e_k}\big|_{s} - \Delta A^{e_k} \tag{10}$$

Subsequently, $A_{uc}^{e_k}\big|_{s+1}$ is set to zero for all elements where Equation 4 is met. All elements with $A_{uc}^{e_k} = 0$ are considered to be failed. Finally, the number of cycles is updated:

$$N|_{s+1} = N|_{s} + \Delta N_{inc} \tag{11}$$

and the procedure is repeated in the next step. This algorithm was implemented in Abaqus/Standard® 6.14 via the user subroutines UEL and UEXTERNALDB. Further details are provided in reference 7.

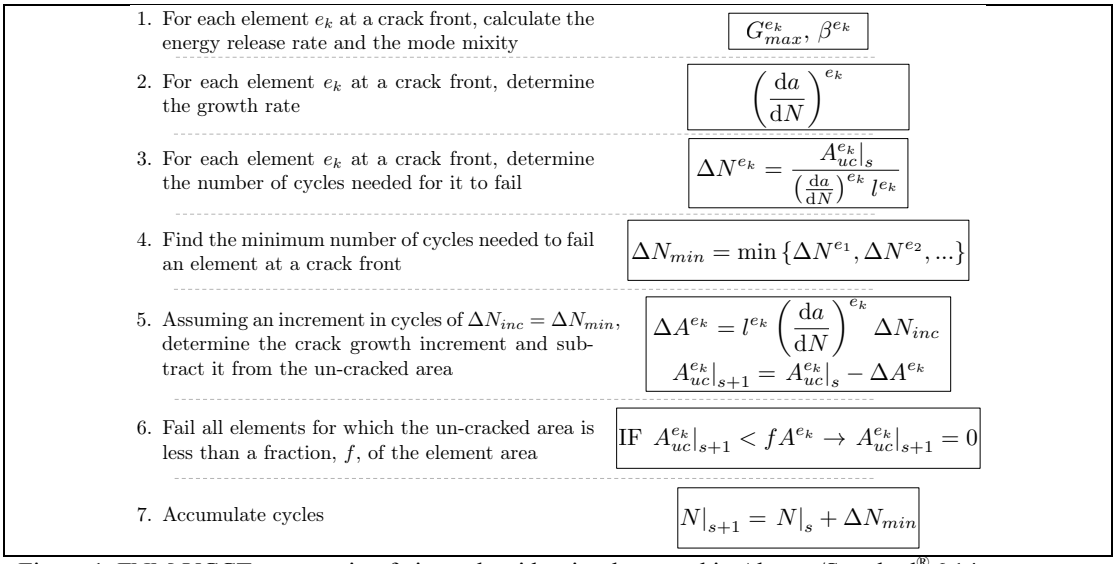

Figure 1. FNM-VCCT propagation fatigue algorithm implemented in Abaqus/Standard® 6.14.

ANALYSIS BENCHMARKING

Existing Benchmark Case For Delamination Growth Predictions Under Pure Mode I Conditions

In a previous study, the development of a benchmark example for delamination growth prediction under cyclic loading was presented in detail [6]. The example was based on two-dimensional (2D) and three-dimensional (3D) finite element models of the Double Cantilever Beam (DCB) specimen shown in Figure 2, which is used for mode I (mixed-mode ratio G_{II}/G_T=0) fracture toughness testing. The benchmark example is independent of the analysis software used and allows for the assessment of the delamination growth prediction capabilities in commercial finite element codes.

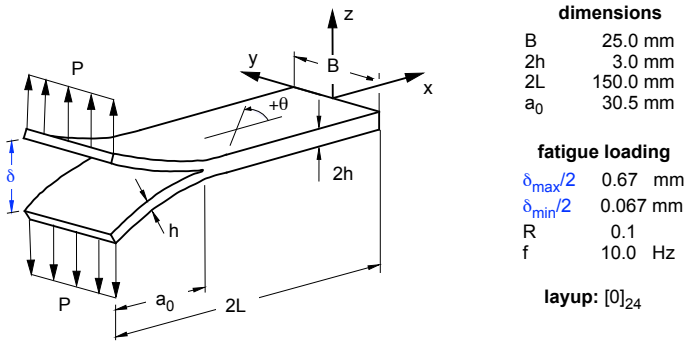

Figure 2. Double Cantilever Beam (DCB) specimen used as mode I benchmark case [6].

For the benchmark case, experimental anomalies such as fiber bridging were not addressed, in order to avoid unnecessary complications. For the creation of the benchmark case, the material data and cyclic loading were selected first. Second, the number of cycles to delamination onset, N_D, was calculated from the fatigue delamination growth onset data of the material. Third, the number of cycles during stable delamination growth, ΔN_G, was obtained incrementally from the material data for fatigue delamination propagation (Paris Law) by using growth increments of Δa=0.1 mm. Fourth, the total number of growth cycles, N_G, was calculated by summing over the increments ΔN_G. Fifth, the corresponding delamination length, a, was calculated by summing over the growth increments Δa. Finally, for the benchmark cases, results for delamination onset and growth were combined, and the delamination length, a, was calculated and plotted versus an increasing total number of load cycles $N_T=N_D+N_G$, as shown in Figure 3. It was assumed that delamination length increase during cyclic loading obtained from finite element analysis should closely match the growth shown in the benchmark example.

The benchmark example was compared to the low-cycle fatigue tool in Abaqus/Standard® [6]. Starting from an initially straight front, the delamination was allowed to grow based on the algorithms implemented into the commercial finite element software. Input control parameters were varied to study the effect on the computed delamination increase during cyclic loading. In general, good agreement between the results obtained from the growth analysis and the benchmark results could be achieved by selecting the appropriate input parameters. Overall, the results for this pure mode I case were encouraging, but it was determined that further assessment for more complex mixed-mode delamination cases was required.

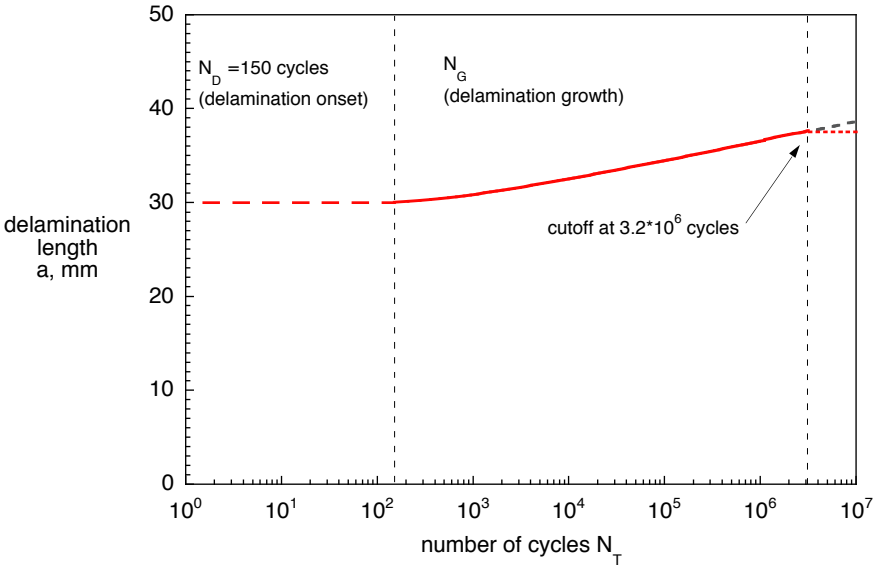

Figure 3. Benchmark curve for pure mode I condition [6].

Development of Benchmark Cases for Delamination Growth Predictions Under Mixed-Mode I/II Conditions

To allow further assessment, new benchmark examples were created for delaminations under mixed-mode conditions. For the current numerical investigation, the Mixed-Mode Bending (MMB) specimen, as shown in Figure 4, was chosen, since it is simple, and had been used previously to develop an approach to assess the quasi-static delamination propagation simulation capabilities in commercial finite element codes [9].

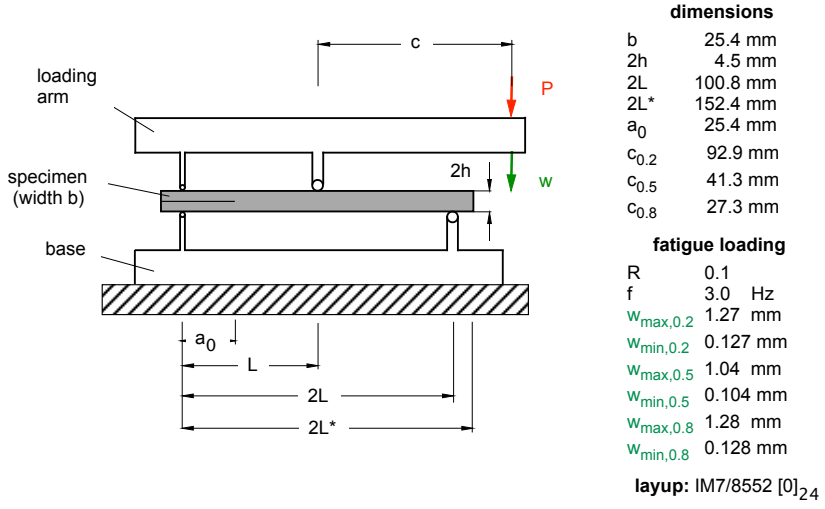

Figure 4. Mixed-mode bending specimen.

Three configurations of the MMB specimen were studied, to produce results at mixed-mode ratios G_{II}/G_T =0.2, 0.5, and 0.8. Specimens made of IM7/8552 graphite/epoxy with a unidirectional layup, $[0]_{24}$, were modeled. The material, layup, and overall specimen dimensions, including initial crack length, a, are shown in

Figure 4, and were identical to the specimens analyzed earlier in [9]. Additional parameters (e.g., growth law, frequency, load level, R-ratio) were taken from a recent experimental study [10] where MMB specimens were tested to obtain the mixed-mode fatigue delamination growth characteristics of a IM7/8552 graphite/epoxy tape laminate.

FINITE ELEMENT MODEL

For the current study, an MMB specimen made of IM7/8552 graphite/epoxy with a unidirectional layup, $[0]_{24}$, was modeled. The material properties were taken from a previous study [9]. An example of a two-dimensional finite element model of an MMB specimen with boundary conditions is shown in Figure 5a for a mixed-mode ratio G_{II}/G_T =0.5.

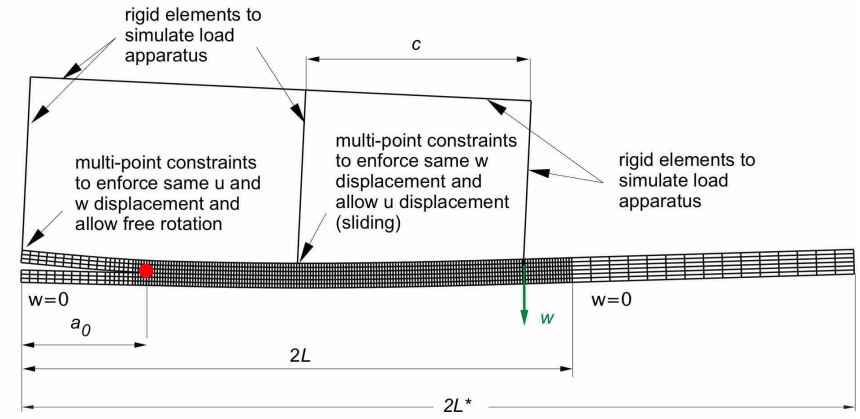

(a). *2D FE model (G_{II}/G_T=0.5, c=41.3 mm).*

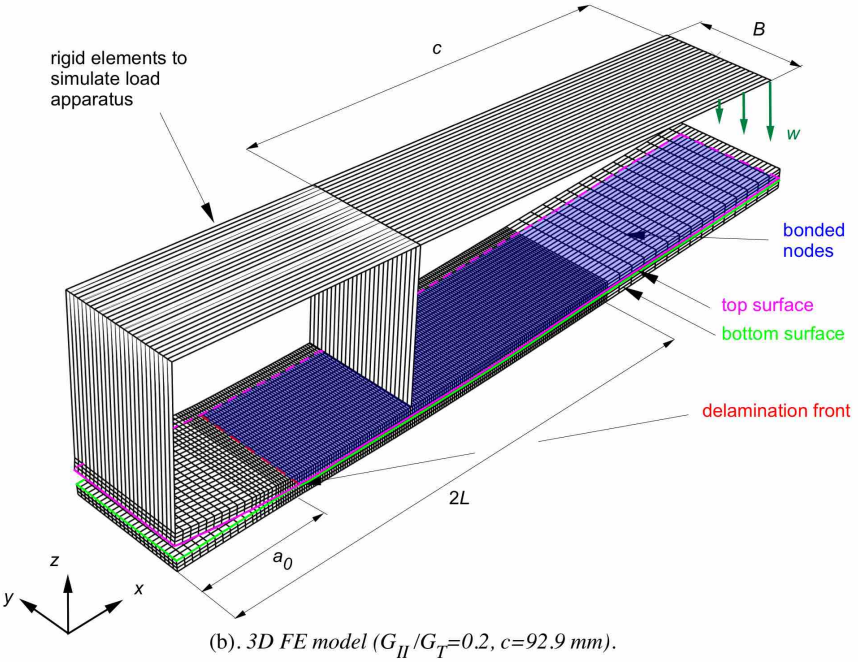

(b). *3D FE model (G_{II}/G_T=0.2, c=92.9 mm).*

Figure 5. Examples of finite element models used to simulate MMB specimens.

Based on previous experience [9], the specimen was modeled with solid plane strain elements (CPE4I) in Abaqus/Standard® 6.14 to create the benchmark cases. The MMB specimen was modeled with six elements through the specimen thickness. Along the length, all models were divided into different sections with different mesh refinement. The resulting element length at the delamination tip was Δa=0.5 mm. The load apparatus was modeled explicitly using rigid beam elements (R2D2) as shown in Figure 5a. Multi-point constraints were used to connect the rigid elements with the planar model of the specimen and enforce the appropriate boundary conditions.

An example of a three-dimensional finite element model of the MMB specimen is shown in Figure 5b for a mixed-mode ratio G_{II}/G_T =0.2. Along the length and through the thickness, the 3D mesh was identical to the one described above for the 2D model. Across the width, a uniform mesh (25 elements) was used to avoid potential problems at the transition between a coarse and finer mesh [9]. The specimen was modeled with solid brick elements (C3D8I), which had yielded excellent results in previous studies [6]. The load apparatus was modeled explicitly using rigid plate elements (R3D4) as shown in Figure 5b. As before, for the two-dimensional model, multi-point constraints were used to connect the rigid elements with the solid model of the specimen and enforce the appropriate boundary conditions.

For all 2D and 3D models, the plane of delamination was modeled as a discrete discontinuity in the center of the specimen. For the analysis with Abaqus/Standard® 6.14, the models were created as separate meshes for the upper and lower part of the specimens, with identical nodal point coordinates in the plane of delamination. Two surfaces (top and bottom surface) were defined to identify the contact area in the plane of delamination as highlighted in Figure 5b. Additionally, a node set was created to define the intact (bonded nodes) region. The mesh of the specimen was kept the same for all three mode ratios. Only the length, *c*, of the rigid elements used to simulate the load apparatus was changed, as shown in Figure 5.

DEVELOPMENT OF BENCHMARK CASES FOR 20%, 50% AND 80% MODE II

For the development of the MMB benchmark cases for delamination onset from an initial flaw, and subsequent growth under cyclic loading, guidance was taken from test results for mixed-mode interlaminar fracture toughness and fatigue characterization [10]. The fatigue tests at each mode ratio were performed under constant amplitude load control (load ratio R=0.1, f=3 Hz) at load levels that caused the energy release rate at the front, G_{max}, to reach values of 60%, 50%, 40% and 30% of G_c. Here, G_c is the fracture toughness at the corresponding mixed-mode ratio, which can be obtained from static fracture toughness data (see Table I). The current study focused on the case for 60% G_c.

For the benchmark creation, the steps discussed in detail in previous studies [6] were followed. First, the fracture properties for IM7/8552 were determined and w_{max} and w_{min} corresponding to the maximum and minimum displacement values during constant amplitude loading were calculated (see Figure 4 and Table I). These values were used to create the benchmark examples in the current study.

Second, the number of cycles to delamination onset, N_D, was calculated from the delamination onset curve, which is a power law fit

$$G = m_0 \cdot N_D^{m_1} \tag{12}$$

of the experimental data [10]. The values for m_0 and m_1 are listed in Table I. Since composites do not exhibit the same threshold behavior commonly observed in metals, a cutoff value, G_{th}, below which delamination growth was assumed to stop, was projected from the experimental data [10] and listed in Table I.

Third, the number of cycles during delamination growth, N_G, was obtained from the fatigue delamination propagation relationship (Paris Law), equation (1). The factor c and exponent n, in equation (1), were obtained by fitting the curve to the experimental data [10], which had been converted to SI-units (see Table I).

TABLE I. FRACTURE PROPERTIES

IM7/8552 Fracture Toughness Data [9]			
G_{Ic} = 0.212 kJ/m^2	G_{IIc} =0.774 kJ/m^2		η= 2.1
IM7/8552 Delamination Growth Onset Data [10]			
$\boldsymbol{G_{II}/G_T}$ **= 0.2**	m_0=0.304	m_1= -0.09	G_{th} = 0.06 kJ/m^2
$\boldsymbol{G_{II}/G_T}$ **= 0.5**	m_0=0.383	m_1= -0.103	G_{th} = 0.06 kJ/m^2
$\boldsymbol{G_{II}/G_T}$ **= 0.8**	m_0=0.523	m_1= -0.125	G_{th} = 0.06 kJ/m^2
IM7/8552 Delamination Growth Rate Data (Paris Law) [10]			
$\boldsymbol{G_{II}/G_T}$ **= 0.2**	*c=2412*	*n=8.4*	
$\boldsymbol{G_{II}/G_T}$ **= 0.5**	*c=6.79*	*n=5.4*	
$\boldsymbol{G_{II}/G_T}$ **= 0.8**	*c=4.58*	*n=5.1*	
Constant amplitude loading			
$\boldsymbol{G_{II}/G_T}$ **= 0.2**	G_c = 0.227 kJ/m^2	w_{max}=1.27 mm	w_{min}=0.127 mm
$\boldsymbol{G_{II}/G_T}$ **= 0.5**	G_c = 0.323 kJ/m^2	w_{max}=1.04 mm	w_{min}=0.104 mm
$\boldsymbol{G_{II}/G_T}$ **= 0.8**	G_c = 0.543 kJ/m^2	w_{max}=1.28 mm	w_{min}=0.128 mm

For practical applications, equation (1) can be replaced by an incremental equivalent expression

$$\frac{\Delta a}{\Delta N} = c \cdot G_{max}^{n} \tag{13}$$

where for the current study, increments of Δa=0.1 mm were chosen. Starting at the initial delamination length, a_0=25.4 mm, the energy release rates, G_{max}, were obtained for each increment, from a curve fit through previously generated G versus crack length, a, data. These energy release rate values were then used to obtain the increase in delamination length per cycle, or growth rate $\Delta a/\Delta N$, from the Paris Law. The detailed procedure is described in detail in reference 6.

Fourth, the number of cycles during delamination growth, N_G, was then calculated by summing the increments ΔN_i

$$N_G = \sum_{i=0}^{k} \Delta N_i = \sum_{i=0}^{k} \frac{1}{c} G_{i,max}^{-n} \Delta a \tag{14}$$

where k is the number of increments.

Fifth, the corresponding delamination length, a, was calculated by adding the incremental lengths, Δa, to the initial length, a_0,

$$a = a_0 + a^* = a_0 + k \cdot \Delta a \tag{15}$$

where a^* is the increase in delamination length.

Finally, for the combined case of delamination onset and growth, the total life, N_T, may be expressed as

$$N_T = N_D + N_G \tag{16}$$

where, N_D is the number of cycles to delamination onset and N_G is the number of cycles during delamination growth. For all three mixed-mode cases, the increase in delamination length, a^*, was plotted for an increasing number of load cycles, N_T, as shown in Figure 6.

For the first N_D cycles (cycles to delamination onset; horizontal dashed lines), the delamination length remains constant. The onset is followed by a growth section where - over N_G cycles - the delamination length increases following the Paris Law (solid lines). Once a delamination length is reached where the energy release rate drops below the assumed cutoff value, G_{th}, the delamination growth no longer follows the Paris Law (solid lines) and growth stops (horizontal dotted lines). It was assumed that delamination length increase during cyclic loading obtained from finite element analysis should closely match the growth shown in the benchmark example.

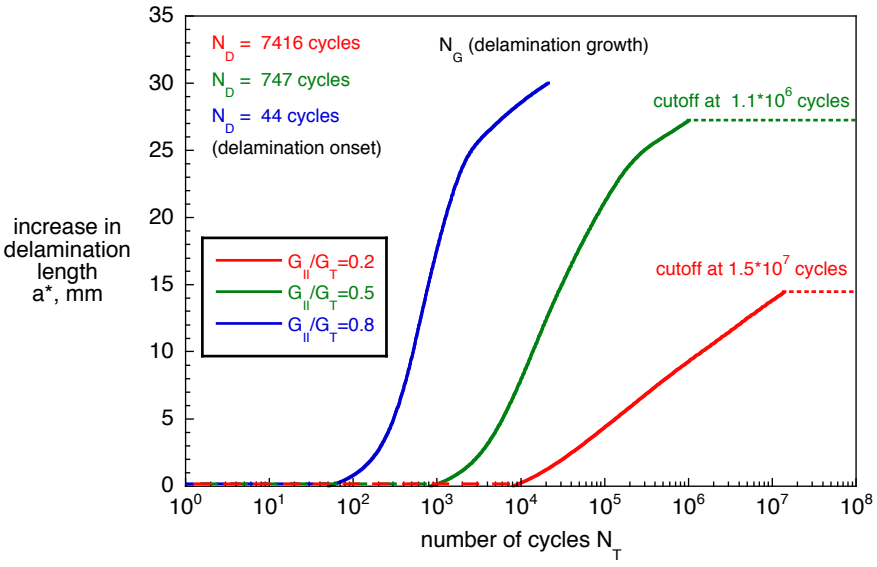

Figure 6. Benchmark curves for mixed-mode I/II conditions.

Automated Delamination Onset and Growth Analysis Under Cyclic Loading

For the automated delamination onset and growth analysis, the low-cycle fatigue analysis tool in Abaqus/Standard® was used to model delamination growth at the interfaces in laminated composites [11, 12]. A direct cyclic approach is part of the implementation and provides a modeling technique to obtain the stabilized response of a structure subjected to constant amplitude cyclic loading. The theory and algorithm to obtain a stabilized response using the direct cyclic approach are described in detail in reference 12. Delamination onset and growth predictions are based on the calculation of the strain energy release rate at the delamination front using VCCT. To determine propagation, computed energy release rates are compared to the input data for onset and growth shown in Table II. The implementation is configured to release at least one element at the interface after the loading cycle is stabilized [11, 12].

TABLE II. INPUT FOR ONSET AND GROWTH ANALYSIS

Constant for all analysis (same units as Table I)			
<GIc>=G_{Ic} = 0.212	<GIIc>=<GIIIc>=G_{IIc} =0.774	<eta>=η= 2.1	<tol>= 0.001
Dependent on mixed-mode ratio (same units as Table I)			
Input parameter	**G_{II}/G_T = 0.2**	**G_{II}/G_T = 0.5**	**G_{II}/G_T = 0.8**
<c1>=$(1/m_0)^q$; q=$1/m_1$	1.8E-06	9.E-05	5.6E-03
<c2>=$1/m_1$	-11.1	-9.71	-8.0
<c3>=c (from Paris law)	2412	6.79	4.5788
<c4>=n (from Paris law)	8.4	5.4	5.1
<r1>=G_{th}/G_c	0.264	0.186	0.11
<r2> limit of Paris Law =0.9 G_c	0.9	0.9	0.9

Abaqus/Standard® input file

```
...
*** amplitude definition ****
*AMPLITUDE,name=test, DEFINITION=PERIODIC
1,18.85,0.,0.55
0,0.45
...
*STEP, INC= 10000
*** fatigue analysis ***
*DIRECT CYCLIC,fatigue
 0.005,0.33,,,25,25,,20
,,20000000,,
*DEBOND,SLAVE=VCCT_TOP,MASTER=VCCT_BOT,FREQ=1
*FRACTURE CRITERION,TYPE=fatigue,MIXED MODE BEHAVIOR=BK,
TOLERANCE=<tol>
<c1>,<c2>,<c3>,<c4>,<r1>,<r2>,<GIc>,<GIIc>,
<GIIIc>,<eta>
*** run analysis first with default values
*CONTROLS,type=direct cyclic
,100,5.E-3,100,5.E-3
```

For automated delamination onset and growth analyses, it was assumed that the computed behavior should closely match the benchmark results created below. For all analyses, the elastic constants (given in Table I), the input to define the fracture criterion (given in Table II), and the parameters for delamination onset and delamination growth (Paris Law; given in Table II) were kept constant. The parameters to define the load frequency (f=3 Hz) and the load ratio (R=0.1), as well as the minimum and maximum applied displacement (w_{min} and w_{max}) were also kept constant during all analyses. Based on discussions with a Simulia engineer [13], it was decided to use the input shown in Table II (Abaqus/Standard® input file) for all analyses, to streamline the analysis and reduce the previously reported long analysis time [6]. Further details about the required input parameters and their influence on results are discussed in detail in previous studies [6].

ASSESSMENT OF RESULTS FROM AUTOMATED GROWTH ANALYSES

Results obtained from the Abaqus/Standard® 6.14 low-cycle fatigue analysis tool and those obtained from the user element (FNM-VCCT) were compared to the benchmark results discussed above. For analyses using the low-cycle fatigue implementation in Abaqus/Standard®, 2D and 3D models identical to those discussed in reference 6 were used for the DCB specimen. For analyses of the MMB specimens, the models shown in Figure 5 were used. For the FNM-VCCT analysis, the same 3D models were used, except that the elements immediately above and below the mid-plane were replaced by single extended-interface elements. Native Abaqus/Standard® elements (C3D8) were used everywhere else in the model. The boundary conditions, including loading rig, were identical to those used in the benchmark models. For automated delamination onset and growth analyses, it was assumed that the computed behavior should closely match the benchmark results.

In Figure 7, results are shown for the DCB benchmark case where the total delamination length, a, is plotted versus the total number of cycles, N_T.

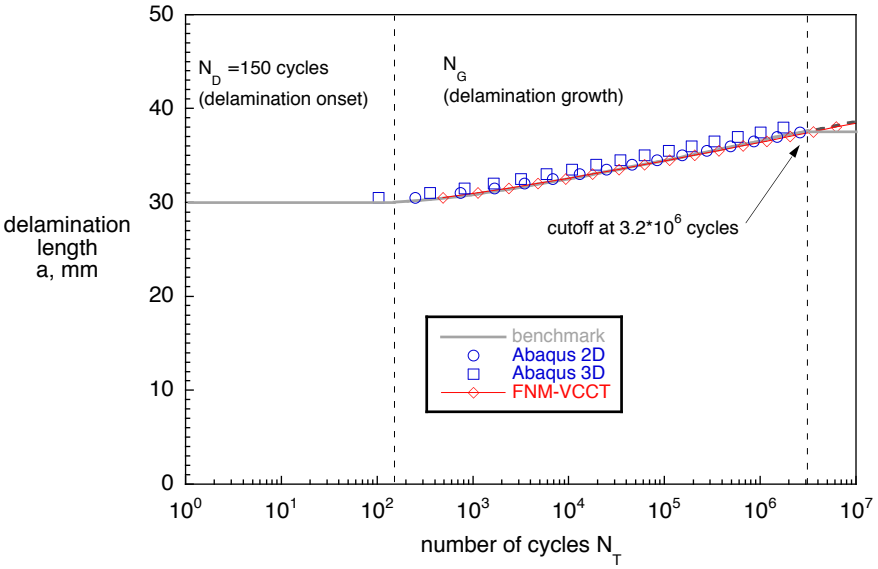

Figure 7. Computed delamination onset and growth for DCB specimen.

For the 3D models, the center of the specimen across the width (at y=b/2) was used as a reference to determine the delamination length. Previous analyses [6] were repeated in Abaqus/Standard® 6.14 with the same fracture input parameters used previously [6]. However, based on discussions with a Simulia engineer [13], it was decided to use the input shown in Table II for `*DIRECT CYCLIC`, to streamline the analysis and reduce the previously reported long analysis time [6]. The results obtained for 2D (open red blue circles) and 3D (open blue squares) were in excellent agreement with the benchmark results (solid grey line). For the results from the user element (FNM-VCCT), the number of cycles to delamination growth onset (N_D=150 cycles) was added to the computational results, since the FNM-VCCT currently does not account for onset. Not only are results shown (red diamonds) in excellent agreement with the benchmarks, they were also obtained at a fraction of the analysis time, as will be discussed below.

In Figure 8, the increase in delamination length, a^*, is plotted versus the total number of cycles, N_T, for different models of the MMB specimen. For the 20% mode II case, the results obtained from the Abaqus/Standard® 2D model (open red circles) qualitatively follow the benchmark (dashed red line), but are shifted towards higher number of cycles, as shown in Figure 8. This shift indicates that the predicted onset occurs at a higher cycle count than that expected from the benchmark. Similarly, the results obtained from the 3D model (open red squares) qualitatively follow the benchmark, but are shifted towards a lower number of cycles. This shift indicates that the predicted onset occurs at a lower cycle count than that expected from the benchmark. For the results from the user element (FNM-VCCT), the number of cycles to delamination growth onset (N_D=7416 cycles) was added to the computational results, since the FNM-VCCT currently does not account for onset. The results (red diamonds) are in excellent agreement with the benchmarks and were obtained at a fraction of the analysis time, as will be discussed below.

For the 50% mode II case, the results obtained from the Abaqus/Standard® 2D models (open green circles) at $N_T < 10^4$ and 3D models (open green squares) were in excellent agreement with the benchmark results (dashed green line), as shown in Figure 8. However, the results obtained from the 2D model started deviating from the benchmark after about 10,000 cycles (crack growth of approximately 12 mm). This deviation was not observed for the results obtained from the 3D model. For the results from the user element (FNM-VCCT), the number of cycles to delamination growth onset (N_D=747 cycles) was added to the computational results, since the FNM-VCCT implementation currently does not account for onset. The results (green diamonds) are in excellent agreement. The threshold cutoff, where delamination growth is terminated and the delamination length remains constant, is not predicted, since the FNM-VCCT implementation currently does not account for this cutoff. The FNM-VCCT analysis was completed at a fraction of the time compared to Abaqus/Standard® analysis, as will be discussed below.

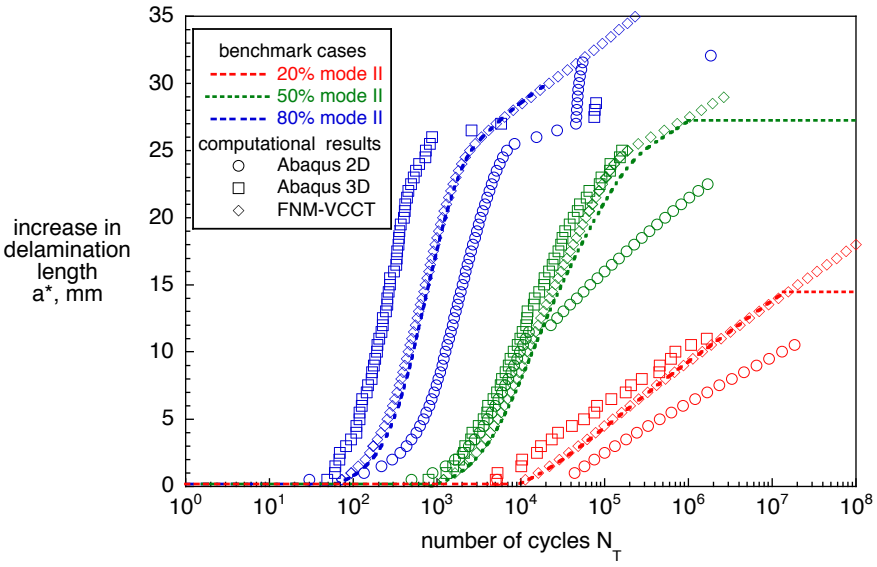

Figure 8. Computed delamination onset and growth for MMB specimens.

For the 80% mode II case, the results obtained from the Abaqus/Standard® models were added to Figure 8 and show the same trend as the results for the 20% mode II. Qualitatively, the results follow the benchmark (dashed blue line), but for the 2D model (open blue circles), they are shifted towards higher number of cycles, and for the 3D model (open blue squares), they are shifted towards lower number of cycles, as shown in Figure 8. This shift indicates that the predicted onset occurs at lower (for 3D models) or higher (for 2D models) cycle counts than that expected from the benchmark. For growth beyond $a^*=25$ mm, the results start to deviate significantly from the trend given by the benchmark. For the results from the user element (FNM-VCCT), the number of cycles to delamination growth onset (N_D=44 cycles) was added to the computational results, since the FNM-VCCT currently does not account for onset. The results (blue diamonds) are in excellent agreement and were obtained at a fraction of the analysis time, as will be discussed below.

The results obtained from the Abaqus/Standard® 6.14 for the MMB benchmark cases may be improved by changing the input parameters for `*DIRECT CYCLIC`. An improvement, however, may likely come at the expense of computational efficiency. This should be examined further. The results from the user element (FNM-VCCT) were in excellent agreement for all benchmark cases for delamination growth and were obtained at a fraction of the analysis time, as shown in Figure 9. The FNM-VCCT currently does not account for onset and the threshold cutoff. The user total CPU time required to compute delamination growth over 2,000,000 cycles is about two orders of magnitude less for FNM-VCCT compared to Abaqus/Standard®. Note that the FNM-VCCT is implemented as a user element, which is most likely less than optimal compared to an in-house algorithm implemented by experienced developers. Since both the FNM-VCCT implementation and the native low cycle fatigue analysis in Abaqus/Standard® use VCCT to compute the energy release rate and also use Paris Law to determine delamination growth, the source of the increase in CPU time must be in the details for the Abaqus/Standard® implementation. The most likely cause is the current low-cycle fatigue analysis tool. Thus, a time efficient delamination growth algorithm in Abaqus/Standard® should be possible, if delamination growth based on node release is made independent of the current low-cycle fatigue analysis tool.

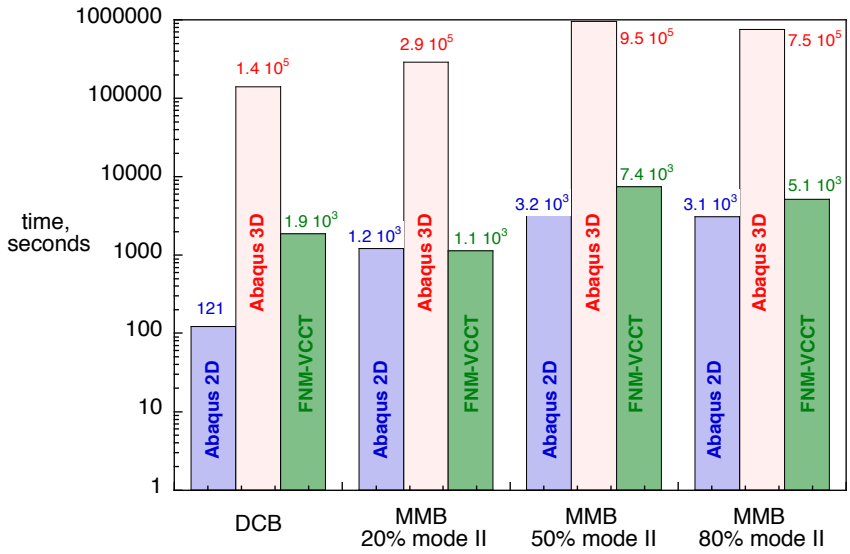

Figure 9. Total CPU time required for different models and implementations.

SUMMARY AND CONCLUSIONS

Analysis benchmarking was used to find time-efficient approaches and algorithms that are suitable for automated delamination growth analysis. First, the Floating Node Method (FNM) was introduced and its combination with a simple exponential growth law (Paris Law) and VCCT was discussed. Implementation of the method into a user element (UEL) in Abaqus/Standard® was also presented. For the assessment of growth prediction capabilities, an existing benchmark case based on the DCB specimen was briefly summarized. Additionally, the development of new benchmark cases, based on the MMB specimen, to assess the growth prediction capabilities under mixed-mode I/II conditions, was discussed in detail. A comparison was presented, in which the benchmark cases were used to assess the existing low-cycle fatigue analysis tool in Abaqus/Standard® in comparison to the FNM-VCCT fatigue growth analysis implementation.

The results showed the following:

- Analysis benchmarking was successfully used to assess the performance of a particular implementation.
- The results from the low-cycle fatigue analysis tool in Abaqus/Standard® were in excellent agreement with the DCB benchmark case.
- Using the same input settings for the low-cycle fatigue analyses of the MMB cases, good results could only be obtained for the 50% mode II case. For the 20% and 80% mode II cases, only the trends could be captured correctly. For longer crack growth length, additional deviations were observed.
- The results obtained from FNM-VCCT were in excellent agreement with all the benchmark cases for delamination growth and were obtained at a fraction of the analysis time.
- A comparison of user total CPU time suggests that a time efficient automated fatigue delamination growth algorithm in Abaqus/Standard®

should be possible by making delamination growth based on node release independent of the current low-cycle fatigue analysis tool.

Overall, the results are promising and the current findings concur with previously published conclusions [6]. Assessing the implementation of two methods in one finite element code illustrated the value of establishing benchmark solutions.

ACKNOWLEDGEMENTS

This research was supported by the Advanced Composites Project as part of NASA's Advanced Air Vehicles Program.

REFERENCES

1. Tay, T. E. 2003. "Characterization and Analysis of Delamination Fracture in Composites - An Overview of Developments from 1990 to 2001,"*Applied Mechanics Reviews,* 56 (1):1-32.
2. Raju, I.S., and T.K. O'Brien. 2008. "Fracture Mechanics Concepts, Stress Fields, Strain Energy Release Rates, Delamination and Growth Criteria," in *Delamination behaviour of composites*, Srinivasan Sridharan ed., Woodhead Publishing in Materials.
3. Rybicki, E. F., and M. F. Kanninen. 1977. "A Finite Element Calculation of Stress Intensity Factors by a Modified Crack Closure Integral," *Eng. Fracture Mech.,* 9:931-938.
4. Krueger, R. 2015. "The Virtual Crack Closure Technique for Modelling Interlaminar Failure and Delamination in Advanced Composite Materials," in *Numerical Modelling of Failure in Advanced Composite Materials*, P. Camanho and S. Hallett, eds., Woodhead Publishing Ltd., pp. 3-53.
5. Krueger, R. 2015. "A Summary of Benchmark Examples and Their Application to Assess the Performance of Quasi-Static Delamination Propagation Prediction Capabilities in Finite Element Codes," *Journal of Composite Materials* 49 (26):3297-3316.
6. Krueger, R. 2010. "Development of a Benchmark Example for Delamination Fatigue Growth Prediction," NASA/CR-2010-216723, NASA Langley Research Center, Hampton, VA, USA.
7. De Carvalho, N. V. and R. Krueger. 2016. "Modeling Fatigue Damage Progression and Onset in Composites Using an Element Based Virtual Crack Closure Technique Combined with the Floating Node Method," in *31st ASC Technical Conference,* Williamsburg, VA, USA.
8. Chen, B. Y., S.T. Pinho, N. V. De Carvalho, P. M. Baiz, and T. E.Tay. 2014. "A Floating Node Method for the Modelling of Discontinuities in Composites," *Engineering Fracture Mechanics* 127: 104-134.
9. Krueger, R. 2012. "Development and Application of Benchmark Examples for Mixed-Mode I/II Quasi-Static Delamination Propagation Predictions," NASA/CR-2012-217562, NASA Langley Research Center, Hampton, VA, USA.
10. Ratcliffe, J. G., and W. M. Johnston Jr. 2014. "Influence of Mixed Mode I-Mode II Loading on Fatigue Delamination Growth Characteristics of a Graphite Epoxy Tape Laminate," presented at the 29th ASC Technical Conference, San Diego, CA.
11. Abaqus Analysis User's Guide. 2014. Abaqus® 6.14, DSS Corp., Providence, RI, USA.
12. Abaqus Theory Manual. 2014. Abaqus® 6.14, DSS Corp., Providence, RI, USA.
13. Sasdelli, M. 2015. Private communication. DSS Corp., Providence, RI, USA.